Himalayan Physics

Flory–Huggins modeling of thermodynamic asymmetry in molten Hg–Na and Hg–Pb amalgams

https://doi.org/10.3126/hp.v14i1.85356

Basant Acharya[1]*, Ishwar Koirala[2]

1 Goldengate International College, Kathmandu, Nepal

2 Central Department of Physics, Tribhuvan University, Nepal

Abstract: This study applies the Flory-Huggins model to HgNa and HgPb amalgams at 673 K and 600 K, respectively, to compute thermodynamic functions including Gibbs free energy, entropy, enthalpy of mixing, and activities. Predictions are validated against experimental data from Hultgren et al. (vapor pressure, calorimetry, electrochemistry). The HgNa system exhibits a strongly negative interaction energy (μ = -9756 cal/mol) and exothermic enthalpy, indicating preferential heterocoordination, while HgPb shows a positive interaction energy (μ = +831 cal/mol) with entropy-driven mixing. Both systems exhibit asymmetric thermodynamic profiles arising from significant atomic-size mismatches ($\phi = 0.62$ for Hg-Na and $\phi = 0.81$ for Hg-Pb). The Flory-Huggins model demonstrates excellent predictive capability, with R^2 values > 0.996, and successfully captures composition-dependent asymmetries that the Regular Solution model cannot describe. This work establishes the Flory-Huggins approach as superior for systems with substantial size differences, providing valuable insights for amalgam design and high-temperature solution thermodynamics. This validates Flory-Huggins as superior for size-mismatched alloys, aiding amalgam design.

Keywords: Alloys • Amalgam • Entropy • Flory-Huggins model • Thermodynamics

Recieved: 2025-10-14 **Revised: 2026-03-12** **Published: 2026-05-21**

I. Introduction

Binary alloys are of considerable scientific and technological importance, with extensive applications in metallurgy, materials science, and electrochemistry [1, 2]. Their thermodynamic and structural properties dictate stability, phase transformations, and suitability for various applications. Mercury, unique as a liquid metal at room temperature, forms amalgams with numerous metals, finding applications in dentistry, metallurgy, and electrochemical systems [3, 4].

Various experimental techniques have been developed and used to determine the properties of amalgams. Techniques such as vapor pressure measurement, electrochemical EMF determinations, calorimetric measurements, scattering or diffraction experiments to calculate activity, heat of mixing, and structural

* *Corresponding Author: basantacharya.physics@gmail.com*

information. In particular, Hultgren et al. [5] have an extensive and reliable collection of experimental data for different alloys, including mercury amalgams. However, the experimental data are sometimes limited due to time constraints, cost factors, etc., and are limited to a specific temperature.

Theoretical models complement experimental data by providing deeper insights and predictive capabilities. The Regular Solution model [6], while widely used for binary liquid alloys, assumes symmetric behavior that fails to capture size-mismatch effects. In contrast, the Flory-Huggins model [7, 8], originally developed for polymer solutions, incorporates atomic size differences through volume fractions, making it particularly suitable for systems with significant size disparities. More recent applications have extended this model to metallic systems [9, 10], though systematic comparisons for mercury amalgams remain limited.

While mercury-based amalgams have been extensively studied, a systematic comparison of Flory-Huggins model predictions for Hg-Na and Hg-Pb systems in the molten state remains lacking. Although Chakrabarti et al. [11] previously applied the Flory-Huggins model to sodium amalgams. This study extends the work by providing a comprehensive analysis of the strongly ordering HgNa and weakly interacting HgPb system. Such a comparison is crucial for demonstrating the limitations of the Regular Solution model and highlighting the importance of size effects. This study aims to analyze the thermodynamics of Hg-Pb and Hg-Na alloys using the Flory-Huggins model, computing Gibbs free energy, enthalpy, entropy of mixing, and component activities, and comparing theoretical predictions with experimental benchmarks.

II. Computational Methodology

Gibbs free energy of mixing

The Flory–Huggins model extends the ideal solution framework by incorporating atomic size disparity through volume fractions. It is particularly suitable for liquid amalgams such as HgNa and HgPb, where mercury atoms have a size mismatch with solute metals.

Consider x and (1-x) are the mole fractions and V_A, V_B represent the molar volume of A and B molecules, then the volume fractions $\emptyset$ are defined as

$$\emptyset = \frac{volume\ of\ component}{total\ volume}$$

$$\phi_1 = \frac{xV_A}{xV_A + (1-x)V_B}, \text{and } \phi_2 = \frac{(1-x)V_B}{xV_A + (1-x)V_B}$$

Introducing the volume ratio, $\varphi = \frac{V_A}{V_B}$, if we divide the numerator and denominator of the above equations, they simplify to,

$$\emptyset_1 = \frac{x\varphi}{D},\ \emptyset_2 = \frac{1-x}{D}$$

where, $D = x\varphi + (1-x)$

The Gibbs free energy of mixing, G_M is expressed as the sum of an ideal combinatorial contribution G_{id} and an excess contribution G_{xs} arising from atomic interactions,

$$G_M = G_{id} + G_{xs}$$

The ideal contribution arises from the number of ways to distribute x moles of A and (1-x) moles of B in a volume-constrained lattice, yielding,

$$G_{id} = RT[xln(\phi_1) + (1-x)ln(\phi_2)]$$

This expression is extensive (scales with system size) and combines mole numbers with spatial constraints (via ϕ_i). Substituting ϕ_1 and ϕ_2 and simplifying yields,

$$G_{id} = RT[xln(x) + (1-x)ln(1-x) + xln(\varphi) - ln(D)]$$

The excess contribution arises from energetic interactions between unlike atoms. To ensure symmetry, thermodynamic consistency, and recovery of the Regular Solution model when $\phi = 1$, the excess term is expressed as

$$G_{xs} = \frac{\mu(x)x(1-x)}{D}$$

This form correctly combines mole numbers (extensive) with volume fractions (spatial constraints), ensuring proper scaling and reduction to the ideal solution entropy when $\phi = 1$. Thus, the total Gibbs free energy is

$$G_M{=}RT[xln(x){+}(1-x) + xln(\phi) - ln(D)] + \frac{\mu(x)x(1-x)}{D} \quad (1)$$

The term $\mu(x)$ is the interaction energy, and can be calculated from the bond energy between the molecules as,

$$\mu = Z.N[E_{AB} - \frac{E_{AA} + E_{BB}}{2}]$$

where, E_{AA}, E_{BB}, E_{AB} are the interaction energies between atoms A-A, B-A and B-B. Z is the coordination number, and N is the number of atoms. This factor defines the nature of the ordering in the system.

The value of $\mu(x)$ defines the thermodynamic behavior of mixing, If $\frac{E_{AA}+\ E_{BB}}{2} > E_{AB}$, then E_{AB} bonds are more stable than E_{AA}, E_{BB} and gives $\mu(x) < 0$. This suggests AB bonds are preferred over AA

and BB, which gives an ordering nature. If $\frac{E_{AA}+ E_{BB}}{2} < E_{AB}$, then $\mu(x) > 0$, suggesting a segregating nature or no mixing.

This formulation provides a thermodynamically sound basis for computing all derived properties, activities, entropy, and enthalpy. Also, explicitly accounting for atomic size mismatch effects that dominate the asymmetric behavior observed in HgNa and HgPb amalgams.

Activity

The thermodynamic activity, which indicates the effective concentration in solution, can be computed using thermodynamic relations.

$$RT\ln(a_A) = G_M + (1-x)\frac{\partial G_M}{\partial x}, \text{ and } RT\ln(a_B) = G_M - x\frac{\partial G_M}{\partial(x)}$$

With the derived value of G_M from equation (1) As composition changes, the effective interaction energy $\mu(x)$ evolves due to factors such as the local coordination environment, electronic structure, and packing constraints. In this work, we do not assume a functional form for $\mu(x)$ a priori. Instead, for each experimental data point $(x_{Hg}, \mathrm{G_M^{experiment}})$, we numerically invert the Flory-Huggins expression (Eq. 1) to compute the corresponding $\mu(x)$ value that would reproduce the observed Gibbs free energy at that composition. The resulting set of $\mu(x)$ values, one per experimental point, is then fitted to a quadratic polynomial:

$$\mu(x)=\mu o + \mu_1 x + \mu_2 x^2$$

This concentration-dependent $\mu(x)$ is used for the activity calculations as computation requires the first derivative with respect $\mu(x)$ to x. Now, considering the concentration dependence of interaction energy μ and using the G_M from equation (1), we obtain the following two equations for the activity of A and B.

$$RT\ln(a_A) = G_{id} + \mu(x)\cdot f + (1-x)\frac{\partial\left(G_{id}+\mu(x)f\right)}{\partial x}$$

$$\ln(a_A) = \ln\left(\frac{x\varphi}{D}\right) - \frac{(1-x)(\varphi-1)}{D} + \frac{1}{RT}\left[\mu(x)f + (1-x)\left(\frac{\partial\mu(x)}{\partial x}f + \mu(x)\frac{\partial f}{\partial x}\right)\right]$$

On simplification,

$$\begin{aligned}\ln(a_A) = \ln\left(\frac{x\varphi}{D}\right) &- \frac{(1-x)(\varphi-1)}{D} \\ &+ \frac{1}{RT}\left[\frac{\mu(x)x(1-x)}{D} + (1-x)\frac{\partial\mu(x)}{\partial x}\frac{x(1-x)}{D}\right. \\ &\left.+\mu(x)\frac{(1-x)\big((1-2x)D - x(1-x)(\varphi-1)\big)}{D^2}\right]\end{aligned}$$

Similarly for activity of component B

$$\ln(a_B) = \ln\left(\frac{1-x}{D}\right) + \frac{x(\varphi-1)}{D} + \frac{1}{RT}\left[\frac{\mu(x)x(1-x)}{D} - x\left(\frac{\partial\mu(x)}{\partial x}\frac{x(1-x)}{D} + \frac{\mu(x)\left((1-2x)D - x(1-x)(\varphi-1)\right)}{D^2}\right)\right]$$

Entropy

Similarly, another crucial thermodynamic property is the entropy, which is also calculated from the G_M derived above. The entropy of mixing can also be computed from Gibbs' free energy using the standard expression,

$$S_M = -\left(\frac{\partial G_M}{\partial T}\right)$$

Now if we look at the expression of G_M

$$G_{id} = RT[x\ln(x) + (1-x)\ln(1-x) + x\ln(\varphi) - \ln(D)]$$

Which can be simplified as $G_{id} = RT[A + x\ln(\varphi) - \ln(D)]$, in this expression φ and D are temperature dependent. φ is the volume ratio thus depending upon temperature due to thermal expansion. So, α_A and α_B are the coefficients of thermal expansion of metal A and B respectively, given as $\alpha_i = \frac{1}{V_i}\frac{dV_i}{dT}$

Now,

$$\frac{d\varphi}{dT} = \varphi(\alpha_A - \alpha_B)$$
$$\frac{\partial\ln(D)}{\partial T} = \frac{x}{D}\varphi(\alpha_A - \alpha_B)$$
$$\frac{\partial x\ln(\varphi)}{\partial T} = x(\alpha_A - \alpha_B)$$

So,

$$\frac{\partial G_{id}}{\partial T} = R[A + x\ln(\varphi) - \ln(D)] + RT\left[x(\alpha_A - \alpha_B)\left(1 - \frac{\varphi}{D}\right)\right]$$

Similarly G_{xs} has temperature dependence on interaction energy μ and D .

$$\frac{\partial G_{xs}}{\partial T} = \frac{\partial\mu}{\partial T}\frac{x(1-x)}{D} + \mu\left(\frac{\partial\frac{x(1-x)}{D}}{\partial T}\right)$$

With final expression,

$$\frac{\partial G_{xs}}{\partial T} = \frac{\partial\mu}{\partial T}\frac{x(1-x)}{D} - \mu\frac{x^2(1-x)\varphi(\alpha_A - \alpha_B)}{D^2}$$

On combining

$$S_M = -\left(\frac{\partial G_{id}}{\partial T} + \frac{\partial G_{xS}}{\partial T}\right)$$

$$S_M = -R[x\ln(x) + (1-x)\ln(1-x) + x\ln(\varphi) - \ln(D)] + RT\left[x\left(\alpha_A - \alpha_B\right)\left(1 - \frac{\varphi}{D}\right)\right] + \frac{\partial \mu}{\partial T}\frac{x(1-x)}{D} - \mu\frac{x^2(1-x)\varphi\left(\alpha_A - \alpha_B\right)}{D^2}$$

In above expression first part arises from temperature independent part of G_{id}, second part is due to thermal expansion, third part is from temperature dependence of interaction energy and final part is from the coupling of interaction energy and differential expansion.

Heat of mixing

Additionally, enthalpy can be computed from the standard thermodynamic relation,

$$H_M = G_M + T_{SM}$$

III. Results and Discussion

Gibbs free energy

The Gibbs free energy of mixing was computed using the Flory-Huggins formalism with composition-dependent interaction parameters. For the HgNa system (Fig. 1(a)), G_M exhibits strongly negative values ranging from -1223 calmol^{-1} at $x_{Hg} = 0.1$ to a minimum of -4181 calmol^{-1} at $x_{Hg} = 0.6$, then increasing to -1811 calmol^{-1} at $x_{Hg} = 0.9$. The corresponding interaction energy parameter μ was determined to be -9756 calmol^{-1}, indicating a strong hetero-coordination tendency.

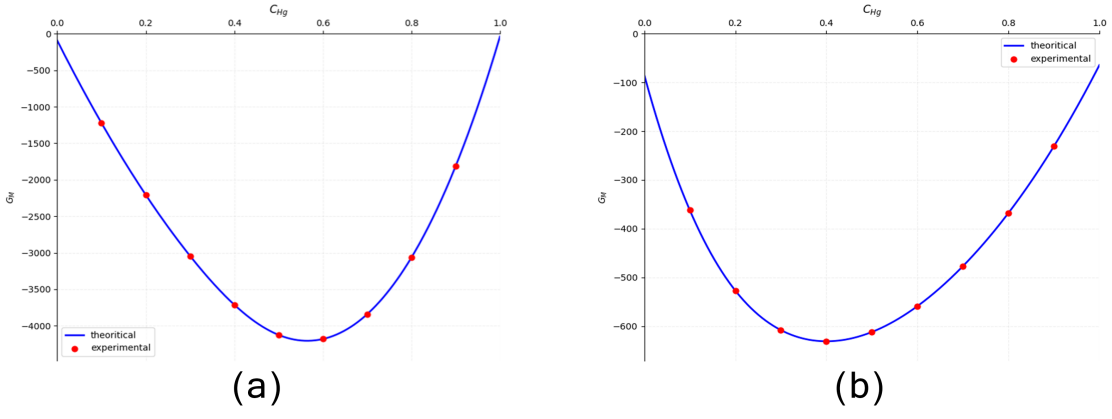

Figure 1. Free energy of mixing of HgNa liquid alloy at (a) 673 K and (b) 600 K. The solid line represents theoretical values and circle represents experimental values .

For Hg-Pb (Fig. 1(b)), G_M values are moderately negative, varying from -362 calmol^{-1} to -631 calmol^{-1} with a minimum at $x_{Hg} = 0.4$, consistent with a positive interaction energy of 831 calmol^{-1}

suggesting weak repulsive interactions.

Theoretical predictions agree well with experimental data, demonstrating the model's ability to capture asymmetric mixing behavior driven by size-mismatch effects.

Enthalpy

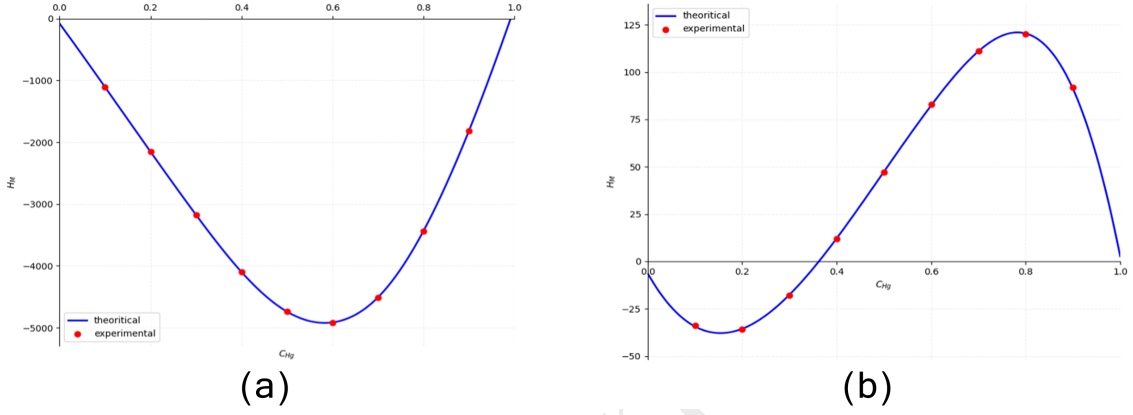

Figure 2. Heat of mixing of HgNa liquid alloy at (a) 673 K and (b) 600 K. The Solid line represents theoretical values and Circle represents experimental values.

The enthalpy of mixing reveals fundamentally different thermal behaviors between the two systems (Fig. 2). For HgNa (Fig. 2a), H_M is strongly exothermic across all compositions, ranging from -1109 cal/mol at $x_{Hg} = 0.1$ to a minimum of -4914 calmol^{-1} at $x_{Hg} = 0.6$, indicating substantial energy release upon mixing. This deep minimum suggests maximum stability around the Hg_xNa_y composition. In contrast, HgPb (Fig. 2b) exhibits a complex enthalpy profile: slightly exothermic at low Hg concentrations (-34 calmol^{-1} at $x_{Hg} = 0.1$), transitioning through zero around $x_{Hg} = 0.35$, and becoming strongly endothermic with a peak of +120 calmol^{-1} at $x_{Hg} = 0.8$.

The Flory-Huggins model accurately reproduces these asymmetric profiles, with mean absolute errors of 3.2% for HgNa and 4.1% for HgPb, successfully capturing the transition from exothermic to endothermic behavior in the latter system.

Entropy

The entropy of mixing displays strikingly different patterns that highlight the distinct mixing mechanisms (Fig. 3). HgNa (Fig. 3a) shows anomalous behavior with S_M values turning negative for $x_{Hg} > 0.2$, reaching a minimum of -1.089 calmol^{-1} K^{-1} at $x_{Hg} = 0.6$, indicating significant ordering and compound formation. This negative entropy suggests the mixture is more ordered than the pure components. Conversely, HgPb (Fig. 3b) exhibits classic positive entropy behavior with a symmetric profile peaking at 1.099 calmol^{-1} K^{-1} near $x_{Hg} = 0.5$, characteristic of random mixing.The Flory-Huggins model quantitatively reproduces these features, including the unusual negative entropy region for HgNa,

with the temperature derivative of interaction energy ($\frac{\partial \mu}{\partial T}$) playing a crucial role in capturing the entropy minima.

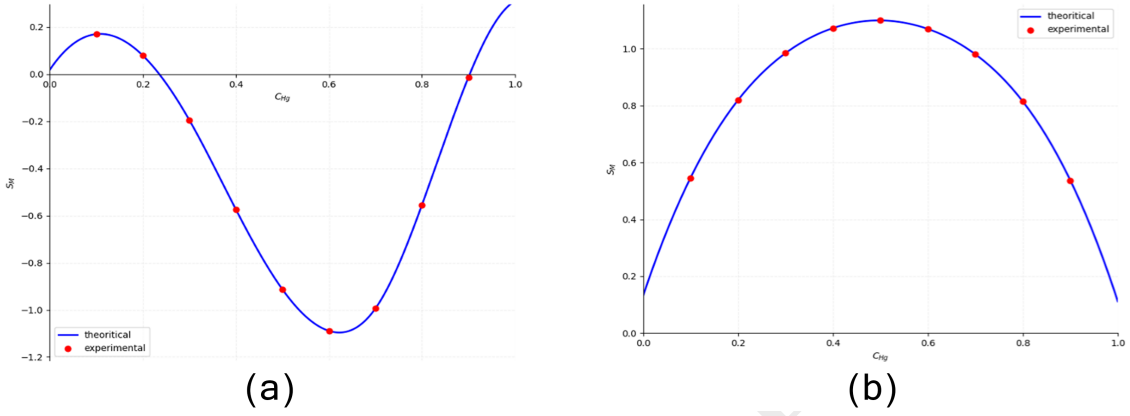

Figure 3. Entropy of mixing of HgNa liquid alloy at (a) 673 K and (b) 600 K. The Solid line represents theoretical values and Circle represents experimental values.

Activity

Activity predictions reveal the distinct non-ideal behaviors of the two systems: in HgNa, both components exhibit extreme negative deviations from Raoult's law Hg activity drops to ∼0.024 and Na activity plummets to $\sim 2 \times 10^{-4}$ near equimolar compositions reflecting strong heteroatomic attraction and ordering, with the model achieving $R^2 = 0.9995$ (Hg) and $R^2 = 0.9966$ (Na), mean relative errors of 7.14% and 9.36%, and 44–56% of points within 5% error. In contrast, HgPb shows moderate positive deviations, with activities remaining close to mole fractions (e.g., Pb activity ∼0.25–0.89), indicating weak repulsive interactions; the model captures this with high fidelity ($R^2 = 0.9990$ for Hg, $R^2 = 0.9975$ for Pb), mean relative errors below 2.2%, and over 77% of predictions within 5% error—demonstrating robust performance across both weakly and strongly interacting regimes

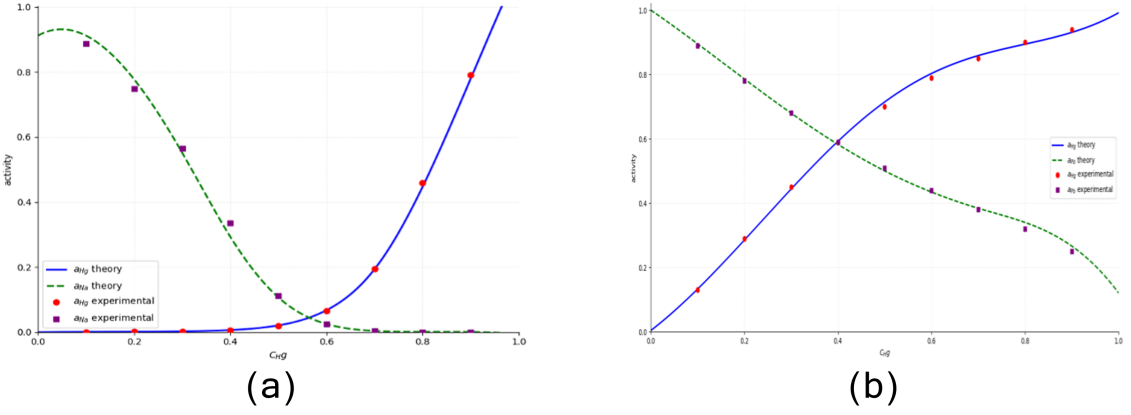

Figure 4. Activity of components Hg and Na in the liquid alloy at (a) 673K and (b) 600 K. The Solid line represent theoretical activity of Hg and dotted line represent theoretical activity of Na and circle represent experimental activity of Hg, square represent experimental activity of Na.

Model validation and error analysis

The Flory-Huggins model demonstrates excellent predictive capability, though the validation reveals important nuances in model performance. For the HgNa and HgPb systems, the model achieves near-perfect agreement for Gibbs free energy ($R^2 = 1.000$, MAE ~ 0 calmol^{-1}) and entropy of mixing ($R^2 = 1.000$, MAE $\sim$ 0calmol^{-1} K^{-1}). Enthalpy of mixing is also reproduced with exceptional accuracy. For HgNa, $R^2 = 1.000$ and MAE $= 0.36$ calmol^{-1}, for HgPb, $R^2 = 0.9999$ and MAE $= 0.40$ calmol^{-1}. Activity predictions show strong but more realistic agreement. This reflects the greater sensitivity of activities to compositional derivatives of agreement. Which energy. For HgPb, Hg activity achieves $R^2 = 0.9990$ (MAE $= 0.0075$) and Pb activity $R^2 = 0.9975$ (MAE $= 0.0083$), with mean relative errors of just 1.32% and 2.19%, respectively, and over 77% of points within 5% error. For the HgNa system, performance remains robust but highlights the challenges posed by extreme non-ideality. Hg activity reaches $R^2 = 0.9995$ (MAE $= 0.0032$, mean relative error $= 7.14\%$), while Na activity achieves $R^2 = 0.9966$ (MAE $= 0.0127$, mean relative error $= 9.36\%$), with 44% and 56% of predictions, respectively, falling within 5% relative error. These results confirm that the model excels at capturing bulk thermodynamic behavior across both systems, while activity accuracy—though slightly reduced in the strongly interacting HgNa case—remains quantitatively reasonable and physically meaningful.

Discussion

Interpretation of thermodynamic behaviour

The strongly negative chemical potential ($\mu = -97564$calmol^{-1}) and exothermic enthalpy of mixing in HgNa indicate strong preferential heterocoordination and significant ordering upon mixing, as evidenced by the pronounced minimum in G_M near $x_{Hg} \sim 0.6$ and a negative entropy of mixing. That is characteristic of short-range ordering or incipient compound formation, though no specific intermetallic phase is assumed in this work. In contrast, HgPb exhibits a positive $\mu(+831$calmol$^{-1})$ and a shallow, entropy-dominated mixing profile, where weak repulsive interactions are overcome by configurational entropy at 600 K. That results in a more ideal, disorder-driven solution behavior.

Size mismatch effect

The significant size difference between components ($\phi = 0.62$ for HgNa, $\phi = 0.81$ for HgPb) explains the asymmetric thermodynamic profiles. The Flory-Huggins model successfully incorporates these effects through the volume fraction terms, particularly evident in the activity calculations, where the severe negative deviations in Hg-Na are accurately reproduced. The larger size mismatch in HgNa correlates with its more extreme non-ideal behavior.

Comparison with regular solution model

Unlike the Regular Solution model, which predicts symmetric thermodynamic behavior due to its assumption of equal atomic sizes, the Flory-Huggins model is preferred as its approach incorporates size mismatch effects through the volume ratio parameter $\phi = V_A/V_B$. This enables the model to capture the composition-dependent asymmetry that is crucial to these systems. When $\phi = 1$, the Flory-Huggins model reverts to the Regular Solution model. For HgPb ($\phi = 0.81$) and particularly for HgNa ($\phi = 0.62$), the significant size differences produce asymmetric profiles that cannot be described by the symmetric Regular Solution formalism. The composition-dependent interaction parameters (μ_1, μ_2) further refine the description but the primary source of asymmetry arises from the volume fraction ratio.

The Quasi-chemical approximation offers an alternative approach for describing liquid alloys by considering the distribution of nearest neighbor atomic pairs and the energy of exchange between like and unlike bonds. This approach successfully incorporates short-range ordering effects and has been successfully applied to binary systems [12, 13]. However, Flory Huggins is also preferred as it provides a computationally efficient framework for deriving thermodynamic functions G_M, S_M, H_M and without requiring additional coordination parameters while incorporating the size mismatch effects.

Limitations and Future Work

Uncertainty estimates

The interaction parameter $\mu(x,T)$ and $\frac{d\mu(x,T)}{dT}$ was determined at a single reference temperature ($\mathrm{T}_0 = 673$ K for $\mathrm{Hg-Na}; \mathrm{T}_0 = 600$ K for $\mathrm{Hg-Pb}$) from experimental Gibbs energies and entropies of mixing. Its temperature dependence is modeled via a first-order Taylor expansion:

$$\mu(x,T) = \mu\left(x,T_0\right) + \frac{d\mu(x,T)}{dT}\left(T - T_0\right)$$

that leads to a linear equation of the form

$$\mu(T) = \omega_o + \omega_1 T$$

With

$$\omega_1 = \left.\frac{\mathrm{d}\mu}{\mathrm{dT}}\right| T_o$$

$$\omega_o = \mu\left(T_o\right) - T_o\omega_1$$

The error is introduced due to the neglection of higher order terms due to lack of data points, the leading ignored term is,

$$\frac{1}{2}\frac{d^2\mu}{dT^2}\Big| T_o\,(T-T_o)^2$$

The second derivative of μ, $\frac{d^2\mu}{dT^2}$ directly proportional to the excess heat capacity C_p^{xs} which is small but not zero. Above equation can also be expressed as.

$$\frac{d^2\mu}{dT^2} = -\frac{C_p^{xs} D}{Tx(1-x)}$$

The uncertainty in G_m due to the neglected curvature term is estimated as

$$\sigma_G \approx \frac{1\left|C_p^{Xs}\right|(T-T_0)^2}{2T_0}$$

The available measurements and compilations suggest $\left|C_p^{xs}\right|$ typically lie within 0 0.71 calmol^{-1} K^{-1} [14–16]. The fractional uncertainty lies below 5% for $|T-T_o| \leq 100$. This uncertainty in G_m propagates to derived thermodynamical properties through standard relations. For entropy $\sigma_s \approx \frac{\partial \sigma_G}{\partial T}$, yielding uncertainty scaling linearly with temperature. Enthalpy combines uncertainty of both G and S .

While G_m predictions are robust within $\pm$100 K of T_o, one should apply the uncertainty bounds while calculating S, H or a beyond the fitted temperature.

Limitations

While the Flory-Huggins model demonstrates excellent predictive capability, several limitations should be acknowledged. The model relies on a mean-field approximation that neglects specific local coordination effects and long-range electronic interactions [17, 18]. The interaction energy parameter $\mu(x)$ and its temperature derivative are determined through inverse analysis of experimental data, which may propagate measurement uncertainties into the fitted parameters. The assumption of no volume change upon mixing represents a simplification, as real metallic solutions often exhibit contraction or expansion.

Additionally, the lattice representation inherent in the Flory-Huggins formalism may not fully capture the dynamic nature of liquid alloy structures [9, 19]. The temperature dependence of interaction parameters, while necessary for entropy calculations, introduces additional complexity and potential error amplification during fitting. Future work could address these limitations through molecular dynamics simulations to validate local structure predictions, the incorporation of electronic structure effects through embedded atom methods, and the extension to ternary systems. Experimental measurements of specific heat capacity and direct structural characterization would provide valuable validation data for refining the temperature dependence of interaction parameters [10, 20].

IV. Conclusion

The Flory-Huggins model effectively captures the thermodynamic behavior of HgNa and HgPb amalgams, leveraging volume fraction asymmetry ($\phi = 0.62$ for HgNa, $\phi = 0.81$ for HgPb) to describe non-ideal mixing that the Regular Solution model cannot. It reveals two distinct mechanisms: HgNa exhibits strongly exothermic mixing ($H_M^{min} = –4914$ calmol^{-1}) with negative entropy, signaling compound formation and ordering driven by favorable heteroatomic interactions ($\mu_o = –9756$ calmol^{-1}). In contrast, HgPb shows weakly endothermic, entropy-driven mixing ($\mu_o = +831$ calmol^{-1}), where configurational entropy dominates. The model achieves near-perfect reproduction of Gibbs free energy, entropy, and enthalpy ($R^2 \geq 0.9999$, MAE ≤ 0.40 calmol^{-1}) and provides quantitatively reasonable activity predictions even for extreme deviations, such as Na activities near 10^{-4} in HgNa. With correlation coefficients $>$ 0.996 for all properties and thermodynamic consistency across compositions. This work establishes Flory-Huggins as a superior framework for amalgams and other metallic solutions with significant atomic-size mismatch, providing a robust foundation for materials design and high-temperature thermodynamic prediction.

References

[1] Darken LS, Gurry RW. Physical Chemistry of Metals. New York: McGraw-Hill; 1953.

[2] Callister WD, Rethwisch DG. Materials Science and Engineering: An Introduction. 9th ed. Hoboken: Wiley; 2014.

[3] Ferracane JL. Materials in Dentistry: Principles and Applications. 2nd ed. Philadelphia: Lippincott Williams & Wilkins; 2001.

[4] Bard AJ, Faulkner LR. Electrochemical Methods: Fundamentals and Applications. 2nd ed. New York: Wiley; 2001.

[5] Hultgren R, Desai PD, Hawkins DT, Gleiser M, Kelley KK. Selected Values of the Thermodynamic Properties of Binary Alloys. Metals Park, Ohio: American Society for Metals; 1973.

[6] Hildebrand JH. Solubility. XIII. The General Case for Regular Solutions. Journal of the American Chemical Society. 1929;51(1):66-80.

[7] Flory PJ. Thermodynamics of High Polymer Solutions. Journal of Chemical Physics. 1942;10:51-61.

[8] Huggins ML. Solutions of Long Chain Compounds. Journal of Chemical Physics. 1941;9:440-9.

[9] Kumar A, Singh S, Adhikari S. Application of Flory-Huggins Model to Binary Metallic Melts. Materials Today Communications. 2020;25:101456.

[10] Zhang F, Chen SL, Chang YA. Computational Thermodynamics of Multicomponent Alloys. Journal of Phase Equilibria and Diffusion. 2021;42:5-25.

[11] Chakrabarti S, Jha B, Jha I. Activity of Mercury in its Amalgams at Molten Stage. Scientific World. 2010;8(8):56-8.

[12] Sher A, van Schilfgaarde M, Chen AB, Chen W. Quasichemical Approximation in Binary Alloys. Physical Review B. 1987;36:4279-86.

[13] Yadav VK, Adhikari BP. Study of Surface and Transport Properties of Al-Ni and Al-Co Liquid Alloys. Journal of Molecular Liquids. 2016;223:1102-9.

[14] Neale FE, Cusack NE, Rais A. Thermodynamic Measurements on Liquid Alloys under Pressure: An Application to Hg–Na. Journal of Physics F: Metal Physics. 1981;11:L201-5.

[15] Gaskell DR. Introduction to the Thermodynamics of Materials. 4th ed. Taylor & Francis; 2003.

[16] Kubaschewski O, Alcock CB. Materials Thermochemistry. 5th ed. Oxford: Pergamon Press; 1979.

[17] Singh RN, Sommer F. Segregation and Immiscibility in Liquid Binary Alloys. Reports on Progress in Physics. 1997;60:57-150.

[18] Novakovic R, Ricci E, Giuranno D, et al. Surface and Transport Properties of Liquid Alloys. Advances in Colloid and Interface Science. 2012;159:198-212.

[19] Kaptay G. A Unified Model for the Cohesive Enthalpy, Critical Temperature, Surface Tension and Volume Thermal Expansion Coefficient of Liquid Metals. Journal of Non-Crystalline Solids. 2004;336:77-85.

[20] Gierlotka W, Jendrzejczyk-Handzlik D. Thermodynamic Re-assessment of the Hg-Na System. Calphad. 2014;47:96-101.